Firefly Algorithm Assisted Segmentation of Tumor from Brain MRI using Tsallis Function and Markov Random Field

V. Rajinikanth*, N. Sri Madhava Raja*, K. Kamalanand**

*Department of Electronics and Instrumentation Engineering,
St. Joseph's College of Engineering, Chennai 600 119,
Tamilnadu, India (e-mail: rajinikanthv@stjosephs.ac.in, nsrimadhavaraja@stjosephs.ac.in).
**Department of Instrumentation Engineering, M.I.T. Campus,
Anna University, Chennai 600 044, Tamilnadu, India (e-mail: kamalanand@mitindia.edu)

Abstract: Image segmentation plays a vital role in various medical applications for automated disease examination. In this paper, heuristic algorithm assisted approach is proposed to extract the tumor from a two dimensional (2D) magnetic resonance image. The proposed work is segregated into two processing regions, such as pre-processing and post-processing section. In pre-processing, multi-level thresholding is applied for the 2D MR image using the Firefly Algorithm (FA) and Tsallis entropy function to cluster the similar image pixels based on an ideal intensity thresholds. For post-processing section, an image filter is initially considered to eliminate the skull region. The skull stripped image is then segmented into different partitions using Markov Random Field - Expectation Maximization (MRF-EM). This procedure helps to attain three image segments, such as White Matter (WM), Gray Matter (GM) and tumor mass. The proposed method is tested on the MR images acquired using T1, T2 and Flair modalities. Standard image quality measures are considered to analyze the accuracy of pre-processing section. Further, the tumor mass is considered to examine the exactness in post-processing section. The usefulness of the proposed method is tested using the BraTS 2D MRI dataset and achieved better values of Jaccard similarity coefficient, dice similarity co-efficient, sensitivity, specificity and accuracy for all the three modalities. Further, proposed approach is validated against the existing segmentation procedures, such as Otsu + MRF, Kapur's entropy + active contour, seed based region growing, and principal component analysis. The experimental result confirms that, proposed approach is very efficient in extracting the tumor region compared with the other approaches considered in this study. Finally, the significance of proposed procedure is confirmed using the real time clinical dataset obtained from the BERF.

Keywords: Brain MRI; Tumor; Firefly algorithm; Tsallis entropy; Markov random field; Expectation maximization

1. INTRODUCTION

In medical discipline, image segmentation is widely used to divide an image frame into subsets of homogenous sections in order to examine anatomical or pathological sections. This procedure is used in several medical areas, such as cancer diagnosis (Raja et al., 2015), species identification (Manickavasagam et al., 2014), dye concentration analysis (Kamalanand and Ramakrishnan, 2015) and retinal disease modelling (Raja et al., 2012). In general, medical image segmentation is widely adopted to extract an abnormal tissue or lesion from the image frame for disease examination (Abdel-Maksoud et al., 2015; Balafar et al., 2010; Chaddad, 2015; Despotovic et al., 2015; Elazab et al., 2015; Khandani et al., 2009; Larobina et al., 2015; Palani et al.,2016; Rajesh Sharma and Marikkannu, 2015; Yazdani et al., 2015).

Image multi-thresholding is an initial step in the image processing discipline, which helps in separating an image into non-overlapping, homogenous sections enclosing interrelated objects. Imaging literature provides the information about a number of segmentation practices proposed and implemented by the researchers (Agrawal et al., 2013; Sathya and Kayalvizhi, 2010; Tuba, 2015). Image thresholding procedure is categorised as local level threshold and global level threshold. In the local level thresholding, various threshold values are allocated for every portion of the image. For global level thresholding, a single threshold value is assigned to the whole image. During this process, a probability density function of the grey level histogram is used to find the threshold value based on parametric or a nonparametric approach (Akay, 2013).

Parametric approach in image thresholding is complex and time consuming. The final outcome by this procedure is also affected due to the image quality and initial conditions. Hence, non-parametric approaches are widely adopted by researchers to solve gray and colour image segmentation problem (Raja et al., 2014; Rajinikanth and Couceiro, 2015).

In this paper, image multi-thresholding is proposed using maximal entropy criterion, a non-parametric approach. Recent multi-level thresholding works are performed using heuristic algorithms, due to its reduced computational cost (Kai Chen et al., 2016).

From the literature, it can be observed that, image segmentation work is extensively implemented in medical discipline to extract significant information from medical images. Automated tumor segmentation for 2D and 3D brain MR image is one of the key research field for diagnosis and prognosis of diseases (Chaddad and Tanougast, 2016; Jianjun et al., 2012; Lu et al., 2006). Recent work by Christ and Parvathi (2012) presents the existing schemes to segment the tumor from the MRI dataset.

In this paper, Tsallis entropy based global thresholding scheme is considered to segment 2D MR image database. Tsallis entropy criterion was initially proposed in 1988 and is a non-extensive statistical approach, being typically adopted in image processing applications (Tsallis, 1988). The combination of Tsallis function and various heuristic algorithms have been presented over the past years (Raja et al., 2012). The Firefly Algorithm (FA) assisted Tsallis entropy based global thresholding is employed in this paper to pre-process the test image frame.

During the post-processing segmentation work, image is divided into various regions using the Markov Random Field (MRF) approach (Jung and Lee, 2015; Zhang et al., 2001). MRF is a probabilistic method, widely adopted in several segmentation works. It makes use of the spatial information of the image based on Markov process. This process is based on stochastic modelling approach and works well on images with various uncertainties, such as noise, degradation, imprecise information, partial data (Palani et al., 2016). In this paper, the segmentation process is implemented and validated using the 2D MRI existing in BRAINIX and BraTS dataset.

2. METHODOLOGY AND IMPLEMENTATION

This paper mainly focuses on developing a heuristic algorithm based tool to segment the tumor from the two dimensional (2D) Magnetic Resonance (MR) images recorded using the T1, T2 and Flair (F) modalities of BRAINIX and BraTS dataset.

Proposed work is segregated into two processing divisions, such as pre-processing section and post-processing section. Execution of this methodology is depicted in Figure 1. Pre-processing section involves in: optimal multi-thresholding, quality measure computation and skull stripping; and the post-processing section involves in: MRF – MAP generation, tumor segmentation and analysis.
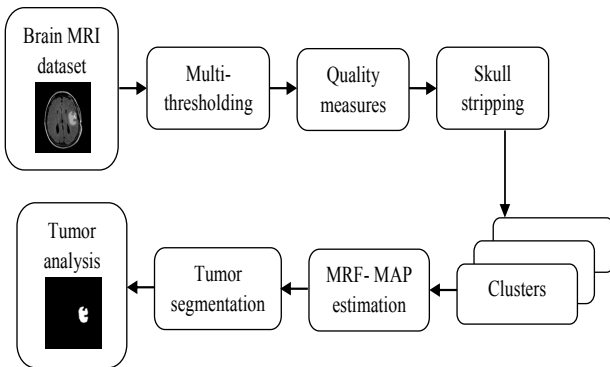

Fig. 1. Structure of the proposed segmentation process.

2.1 Tsallis entropy

In general, the entropy is related with the measure of chaos within a system. Shannon primarily considered the entropy to compute the uncertainty regarding the information content of the system (Bhandari et al., 2015). Shannon also assured that, when a physical system is separated as two statistically free subsystems A and B, then the entropy value can be expressed as:

$$S(A+B) = S(A) + S(B) \qquad (1)$$

Tsallis function can be mathematically expressed as;

$$S_q = \frac{1 - \sum_{i=1}^{T}(p_i)^q}{q-1} \qquad (2)$$

where, T is the system potentials and q is the entropic index (Agrawal et al., 2013; Sathya and Kayalvizhi, 2010).

Eq. (2) will meet the Shannon's entropy when $q \rightarrow 1$.

The entropy value can be expressed with a pseudo additivity rule as:

$$S_q(A+B) = S_q(A) + S_q(B) + (1-q).S_q(A).S_q(B) \qquad (3)$$

Tsallis entropy can be considered to find the optimal thresholds of an image. Consider a given image with L gray levels in the range {0, 1, ..., L-1},with probability distributions $p_i = p_0, p_1, ..., p_{L-1}$.

Tsallis multi-level thresholding can then be expressed as:

$$f(T) = [T_1, T_2, ... , T_k] = argmax$$
$$\left[S_q^A(T) + S_q^B(T) + ... + S_q^K(T) + (1-q).S_q^A(T).S_q^B(T)...S_q^K(T) \right] \qquad (4)$$

where

$$S_q^A(T) = \frac{1 - \sum_{i=0}^{t1-1}\left(\frac{Pi}{P^A}\right)^q}{q-1}, \quad P^A = \sum_{i=0}^{t1-1} Pi$$

$$S_q^B(T) = \frac{1 - \sum_{i=t1}^{t2-1}\left(\frac{Pi}{P^B}\right)^q}{q-1}, \quad P^B = \sum_{i=t1}^{t2-1} Pi$$

$$S_q^K(T) = \frac{1 - \sum_{i=t_k}^{L-1}\left(\frac{Pi}{P^K}\right)^q}{q-1}, \quad P^K = \sum_{i=t_k}^{L2-1} Pi$$

are subject to the following constraints:

$$\left|P^A + P^B\right| - 1 < S < 1 - \left|P^A - P^B\right|$$

$$\left|P^B + P^C\right| - 1 < S < 1 - \left|P^B - P^C\right|$$

$$\left|P^K + P^{L-1}\right| - 1 < S < 1 - \left|P^K - P^{L-1}\right|$$

During this process, the aim is to find the optimal threshold value T which maximizes the objective function $f(T)$. In the proposed work, the threshold value is chosen as $T = 3$ thus the required probability values are P^A, P^B, and P^C. In this work,

the maximization of function *f(T)*, which deals with the segmentation of a given image, is carried using the heuristic algorithm.

2.2 Firefly algorithm

The classical Firefly Algorithm (FA) was initially proposed by Yang (Yang, 2009). FA is a nature inspired meta-heuristic algorithm, in which flashing illumination patterns generated by fireflies are modelled using a suitable mathematical expression.

In the literature, a number of guiding procedures are adopted to enhance the search efficiency of the FA, such as random search, Lévy flight and Brownian walk (Raja et al., 2013). Among the existing methods, it is found that, FA driven by the Brownian walk offers better result in image segmentation application. Hence, in the proposed paper, the recent version of the FA discussed in (Raja et al., 2013; 2014) is considered.

The pseudo code of FA is presented below:

```
START;
    Initialize essential algorithm parameters, D and f(T);
    Generate initial locations of 'n' fireflies for xᵢ (i = 1, 2, … n)
    Determine the intensity of iᵗʰ firefly based on iᵗʰ f(T) value
If  iter < Mᵢₜₑᵣ;
For i = 1,2, … , n;
For j = 1,2, … , n;
    If intensity of firefly j > i,
    Calculate the Cartesian distance and move the i  towards j;
    End if;
    Repeat the above steps until iter = Miter;
    Estimate light intensity and update firefly positions;
End for j;
End for i;
    Sort the fireflies in descending order based on the rank and
    find the optimal value;
End if;
Record the f(T) and optimal threshold values.
STOP;
```

Updated position of a firefly in a *D*– dimensional search can be expressed as;

$$X_i^{t+1} = X_i^t + \beta_0 e^{-\gamma d_{ij}^2} (X_j^t - X_i^t) + \alpha_1 . sign\,(rand - 1/2) \oplus A.|s|^{\alpha/2}$$

(5)

where, X_i^{t+1} is updated position of ith firefly, X_i^t is initial position of ith firefly, $\beta_0 e^{-\gamma d_{ij}^2} (X_j^t - X_i^t)$ is the attraction between fireflies, A is a random variable, β is the spatial exponent, α is the temporal exponent, and $\Gamma(\beta)$ is the Gamma function. The details of FA can be found in the literature. The FA parameters are assigned as; dimension of the search $D = T$; population of firefly is chosen as 30, number of iterations are assigned as 500 and the stopping criteria is the *f(T)*.

2.3 Image quality measures

The pre-processing work is the key step in the proposed segmentation work. Hence, the final outcome of the segmentation process mainly depends on the quality of the thresholded image. The multi-thresholding result is assessed using well known image quality measures, such as the Root Mean Squared Error (RMSE), Normalized Absolute Error (NAE), Peak Signal to Noise Ratio (PSNR), Mean Structural Similarity Index Matrix (MSSIM), Normalized Cross Correlation (NCC) and Structural Content (SC) (Grgic et al., 2004; Wang et al., 2004).

2.4 Skull stripping

Skull stripping is the initial step in the brain image segmentation process. Skull stripping is essential to eliminate the skull and the background area from MRI for quantitative analysis. Skull stripping is normally performed using an image filter which separated the skull and the rest of the image sections by masking the pixels having similar intensity levels. In MR image, generally the skull/bone will have the maximum threshold value (threshold > 200) compared to other brain regions. Hence, the image filter is used to separate the brain regions based on a chosen threshold value. Then by employing the solidity property, the skull is stripped from the brain MRI (Chaddad and Tanougast, 2016).

2.5 Markov random field – Expectation maximization segmentation

Markov Random Field - Expectation Maximization (MRF-EM) is a widely considered methodology for gray scale image segmentation problems.

The MRF-EM can be expressed as follows;

Consider a gray scale test image $I = \{ y(m.n) \,\big|\, 0 \le y \le L-1$. Where y represents the intensity of the image at the pixel location (*m, n*) and L represents the number of threshold levels. During the segmentation process, MRF will approximate the formation of each pixel by mapping into a group of random labels defined as; $X = \{x_1, ... x_N) \,\big|\, x_i \in 1$.

In this paper, the number of labels are assigned as three (since, during the multi-thresholding, *T* value is chosen as three as discussed in section 2.1). Hence, the MRF based segmentation will provide three labels such as white matter, gray matter and tumor. More details regarding the MRF based brain image segmentation are available in (Palani et al., 2016; Zhang et al., 2001)

Implementation of MRF algorithm is defined below:

Step 1: Set the number of labels (*l*) based on number of threshold values (*T*)

Step 2: Formation of cluster classes based on the chosen *l*

$$k_1 = \{ y(m.n) = x_1 \,\big|\, 0 \le y \le t_1$$
$$k_2 = \{ y(m.n) = x_2 \,\big|\, t_1 \le y \le t_2$$
$$k_3 = \{ y(m.n) = x_3 \,\big|\, t_2 \le y \le L-1$$

Step 3: Determine the initial parameter set $\Theta^{(0)}{}_{l}^{l}$ and likelihood probability function $p^{(0)}(f_l|x_l)$.

Step 4: Update the MRF model $x^{(t)}$ such that, the energy function U is minimised.

$$X^* = \underset{x}{arg\,min}\left\{\sum_i\left[\frac{(y_i - \mu_{x_i})^2}{2\sigma^2_{x_i}}ln\,\sigma_{x_i}\right]+\sum_{N_i}V_c(x)\right\} \qquad (6)$$

where, N_i is a four pixel neighbourhood and V_c is the clique potential.

Step 5: Execute the Expectation-Maximization algorithm to update the parameter set $\Theta^{(i)}$ constantly till the log likelihood of $p^{(t)}(f\,|\,x)$ is maximized.

Step 6: Display the labels such as white matter, gray matter and tumor.

2.6 Tumor analysis

The major aim of this work is to extract the tumor region from the 2D brain MR image and to compute the tumor mass associated features for further analysis. In this paper, two types of data, such as brain MRI without the ground truth and brain MRI with the ground truth are considered. For both the cases, the tumor mass is analysed by extracting the key geometric features, such as spread area, major axis length, minor axis length, Equiv. diameter, Solidity and Extent. For the image with the ground truth, the parameters such as normalised are, Jaccard Similarity Coefficient (JSC), Dice Similarity Coefficient (DSC), False Positive Rate (FPR), and False Negative Rate (FNR) are computed (Chaddad and Tanougast, 2016). The mathematical expression is presented below;

$$JSC(I_{gt},I_t) = I_{gt}\cap I_t/I_{gt}\cup I_t \qquad (7)$$

$$DSC(I_{gt},I_t) = 2(I_{gt}\cap I_t)/|I_{gt}|\cup|I_t| \qquad (8)$$

$$FPR(I_{gt},I_t) = (I_{gt}/I_t)/(I_{gt}\cup I_t) \qquad (9)$$

$$FNR(I_{gt},I_t) = (I_t/I_{gt})/(I_{gt}\cup I_t) \qquad (10)$$

where, Igt represents the ground truth image and It stands for the segmented tumor image.

Further, the statistical measures, such as precision, F-measure, sensitivity, specificity and accuracy are also computed (Lu et al., 2004; Moghaddam and Cheriet, 2010).

$$Precision = TP/(TP + FP) \qquad (11)$$

$$F\text{-}measure = 2\,TP/(2\,TP + FP + FN) \qquad (12)$$

$$Sensitivity = TP/(TP + FN) \qquad (13)$$

$$Specificity = TN/(TN + FP) \qquad (14)$$

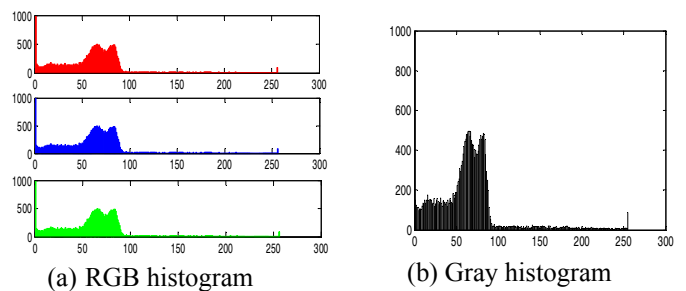$$Accuracy = (TP + TN)/(TP + TN + FP + FN) \qquad (15)$$

where, TP, TN, FP and FN denote the true positive, true negative, false positive and false negative; respectively.

3. RESULTS AND DISCUSSION

This section presents the experimental results of the proposed work. All experiments are carried out in a computer with AMD C70 Dual Core 1 GHz CPU, 4GB of RAM and Matlab R2010a software. The thresholding process is repeated 10 times for each image with threshold *T=3* and the mean value among the trials are recorded as the optimal value. The proposed segmentation procedure is initially implemented on 256 × 256 sized 2D brain MR images (T1, T2, and Flair) available in BRAINIX dataset. Later, the proposed method is validated using 216 x 160 sized brain tumor segmentation database (BraTS-MICCAI challenge). Finally, the clinical significance of the proposed approach is verified using clinical data obtained from the Bharat Education and Research Foundation (BERF).

The segmentation process is initially executed on the MR image of T1modality with slice number 8 ($T1_8$) existing in BRAINIX. It is an RGB image with a pixel size of 256 x 256 and bit depth of 32. The gray version of the RGB image $T1_8$ is considered for the segmentation process. Fig 2 (a) shows the RGB histogram of $T1_8$. Fig. 2 (b) and (c) depicts the histogram of the $T1_8$ gray scale image, before and after the adaptive histogram equalization process. Fig. 3 (a) shows the original $T1_8$ considered in this work. From Fig. 3 (a), one can observe that, the visibility of the T1 modality is poor compared to the T2 and Flair. Hence, the adaptive histogram equalization procedure is applied for all the T1 modality MR images considered in this study ($T1_9$, $T1_{10}$ and $T1_B$). Above said procedure helps to enhance the contrast of the gray test image. The enhanced image is then considered for the multi-thresholding using the FA and Tsallis. The FA based search constantly explores the three dimensional search space (D=*T*=3) till the Objective Function (OF) reaches a maximal value. At the end of the multi-thresholding process, thresholded image is offered by the algorithm (Fig. 3(b)). The quality of the multi-thresholding process is evaluated using the well known image quality measures existing in the literature (Grgic et al., 2004; Wang et al., 2004). Table.2 (a) and (b) shows the image quality measures considered in this work. Fig. 3(c) shows the SSIM map between the original and the thresholded image.

From this expectation maximization map, it can be observed that, the thresholding process enhances the tumor region by grouping the similar pixels. Thresholded image is then applied to an image filter, which separates the skull and soft brain tissue region as shown in Fig. 3(d) and Fig. 3(e). This brain region is then considered for the post-processing work.

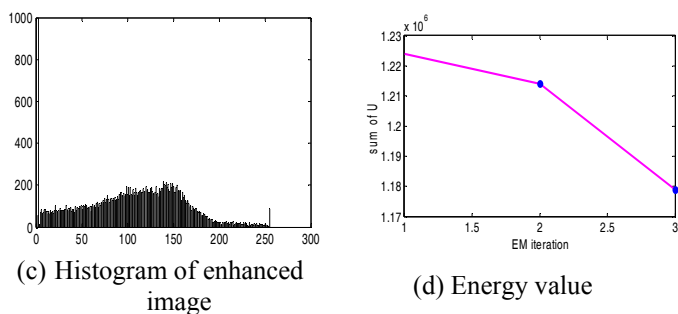(a) RGB histogram   (b) Gray histogram

(c) Histogram of enhanced image

(d) Energy value

Fig. 2. Histogram and the energy value for $T1_8$ MR image.

(a) Test image

(b) Threshold image

(c) SSIM map

(d) Skull

(e) Skull stripped

(f) Random field generation
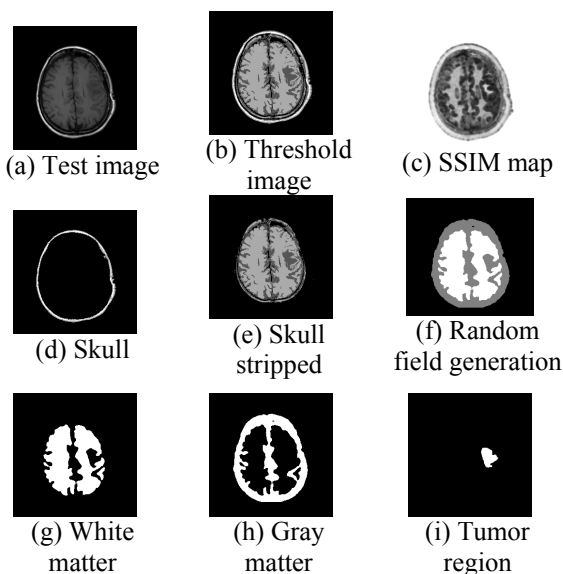
(g) White matter

(h) Gray matter

(i) Tumor region

Fig. 3. Various stage results for T18 brain MR image segmentation process.

Table 1. Segmenttion results for the MR image dataset for T1, T2 and Flair modalities.

	Test image	FA+Tsallis segmentation (T=3)	Skull Stripped brain	Random field generation (l=3)	Extracted region
$T1_9$					
$T1_{10}$					
$T2_8$					
$T2_{10}$					
F_8					
F_{10}					

In the post-processing work, the skull stripped image is considered for the Markov random field generation process for a preferred number of labels (l). In this work, the l is chosen as three and the MRF model is generated by minimizing the energy function U as presented in Fig. 2(d).

After the MRF-MAP generation, the image is separated into various labels, such as white matter (Fig.3 (g)), gray matter (Fig.3 (h)), and the tumor region (Fig.3 (i)). Geometric feature extraction procedure is then applied for the extracted tumor, which offers the tumor mass dimensions in terms of image pixels (Fig.3 (j)).

Table 2 (a). Quality measure values for thresholded image.

Test image	OF	Optimal thresholds	RMSE	NAE
$T1_8$	1.1064	29, 132, 186	20.2663	0.2805
$T1_9$	1.0737	34, 118, 177	24.2829	0.3341
$T1_{10}$	1.0835	26, 140, 182	16.9535	0.2368
$T2_8$	1.3820	30, 125, 160	31.3819	0.5777
$T2_{10}$	1.2248	34, 138, 171	31.1028	0.5427
F_8	1.3004	26, 111, 192	43.0175	0.7736
F_{10}	1.3275	42, 127, 188	41.7133	0.7480
$T1_B$	1.1038	23, 152, 170	33.4952	0.3500
$T2_B$	1.1846	34, 144, 185	39.9465	0.5116
F_B	1.2273	22, 128, 193	26.9228	0.2561

Table 2(b). Quality measure values for multi-thresholded image.

Test image	PSNR (dB)	MSSIM	NCC	SC
$T1_8$	20.2663	0.5324	1.1622	0.7146
$T1_9$	20.4248	0.5299	1.2278	0.6393
$T1_{10}$	23.5456	0.5514	1.0855	0.8202
$T2_8$	18.1972	0.7098	0.7254	1.3342
$T2_{10}$	18.2748	0.7038	0.7597	1.2839
F_8	15.4579	0.6204	0.4056	2.5228
F_{10}	15.7253	0.6039	0.4645	2.1431
$T1_B$	17.6312	0.7755	1.3379	0.5456
$T2_B$	16.1012	0.6691	0.6264	1.8459
F_B	19.5284	0.7857	1.2026	0.6734

Above discussed segmentation procedure is then applied for the MRI gray scale image with various modalities, such as T1, T2 and Flair for the BRAINIX dataset and the outcome of the pre-processing and the post-processing work is presented in Table 1. The pre-processing operation is used to group the pixels based on the chosen threshold (T=3) and the final outcome of the post-processing work offers the tumor existing in the considered test image.

The geometric features (size of tumor) are then extracted and the values are tabulated in Table 3. In this table, the geometric features are recorded based on tumor pixels. In future, these extracted features can be used in the automated classification of tumor, such as benign and malignant.
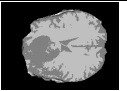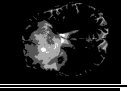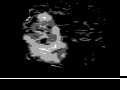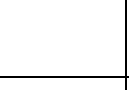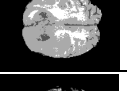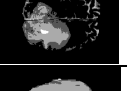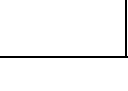
In order to assess the accuracy and clinical significance of the proposed methodology, widely used MRI dataset, BraTS 2012 from multimodal brain tumor segmentation challenge is considered (Kistler et al., 2013; Menze et al., 2015). In this database, the 2D brain MR image doesnot have the skull section, hence it doesnot require the image filtering algorithm to segment the skull. This dataset also has the ground truth (tumor region offered by a radiologist). Hence, the efficiency

of the proposed segmentation process is to be validated against the MR images with ground truth. This dataset has the 2D brain MR images recorded with T1, T2 and Flair modalities. A comparative study between the segmented image and the expert's ground truth will help to evaluate the accuracy and clinical significance of proposed segmentation approach.

Table 3. Geometric feature values for the segmented tumor.

Test image	Area	Major axis length	Minor axis length	Equiv diameter	Solidity	Extent
$T1_8$	869	41.72	29.16	33.26	0.8876	0.6056
$T1_9$	818	46.25	23.45	32.27	0.8872	0.6716
$T1_{10}$	1529	63.61	40.59	44.12	0.7281	0.5560
$T2_8$	1077	45.38	35.40	37.03	0.8134	0.5635
$T2_{10}$	1325	50.23	37.92	41.07	0.8461	0.6760
F_8	1036	45.33	32.10	36.32	0.8691	0.6407
F_{10}	1354	51.41	37.24	41.52	0.8769	0.7319
GT	3880	90.82	64.15	70.29	0.8331	0.5565
$T1_B$	3409	84.46	60.39	65.88	0.8628	0.5939
$T2_B$	3769	85.20	67.09	69.27	0.8000	0.5472
F_B	3865	93.82	63.91	70.15	0.7823	0.5349

Table 4. Segmentation results for the BraTS dataset.

Test image	FA+Tsallis segmentation (T=3)	Ground truth	Segmented tumor
$T1_{100}$			
$T2_{100}$			
F_{100}			
$T1_{120}$			
$T2_{120}$			
F_{120}			

Proposed pre-processing and post-processing works are then implemented on the BraTS MRI dataset and the corresponding results are depicted in table 4. In this study, the slice numbers, 100 and 120 are chosen for the analysis. This table presents the considered image dataset, tri-level thresholded image, ground truth and the extracted tumor from the proposed methodology. From these results, it can be noted that, the shape of extracted tumor from the T1, T2 and

Flair modality based MRI are approximately similar with the corresponding ground truth.

Table 5. Relative result between ground truth and segmented tumor.

Test image	Area (normalized)	JSC	DSC	FPR	FNR
$T1_{100}$	0.9916	0.9260	0.9616	0.0694	0.0098
$T2_{100}$	0.9928	0.9233	0.9601	0.0542	0.0267
F_{100}	0.9936	0.9343	0.9660	0.0473	0.0215
$T1_{120}$	0.8823	0.8186	0.9003	0.0330	0.1544
$T2_{120}$	0.9773	0.8725	0.9319	0.0528	0.0814
F_{120}	0.9538	0.8625	0.9262	0.0776	0.0706

Table 6. Segmentation accuracy measure.

Test image	PRE	F-M	SEN	SPE	ACC
$T1_{100}$	0.9989	0.9955	0.9922	0.9902	0.9912
$T2_{100}$	0.9970	0.9954	0.9939	0.9733	0.9836
F_{100}	0.9975	0.9961	0.9947	0.9785	0.9865
$T1_{120}$	0.9807	0.9874	0.9943	0.8435	0.9158
$T2_{120}$	0.9897	0.9907	0.9918	0.9173	0.9538
F_{120}	0.9910	0.9898	0.9887	0.9285	0.9581

In image segmentation literature, a usual practice is that, the efficiency of proposed segmentation procedure is analyzed using the well known image quantitative measures namely the normalized segmented area, mean error rate, JSC, DSC, FPR and FNR. The statistical measures, such as precision, F-measure, sensitivity, specificity and accuracy are also to be measured to justify the eminence of the proposed segmentation approach (Lu et al., 2004; Moghaddam and Cheriet, 2010). In this paper, the quantitative measures and the statistical measures are computed for the BraTS MRI dataset and the corresponding results are shown in table 5 and 6 respectively.

Table 5 demonstrate that, in all the image cases, the segmented tumor image is closely correlated with the ground truth image and the JSC and DSC are found to be greater than 0.8. Further, the normalised area is found to be high in all the cases. Also by comparing the segmented area with that of the ground truth, it appears that the adopted method is highly efficient in extracting most of the tumor mass irrespective of the modalities. Table 6 confirms that, proposed approach helps to attain better values of precision, F-measure, sensitivity, specificity and accuracy. These results proves that, the proposed segmentation work offers better results for 2D brain MR images recorded with T1, T2, and Flair modalities.

In order to evaluate the performance of proposed technique on complex image cases, three dimensional dataset of BraTS 2013 (pseudo name 0011) presented in Table 7 is considered. Three views of images, such as sagittal, coronal, and axial are extracted using the ITK-SNAP tool developed by

Yushkevich et al. (2006). The proposed work is tested using the slices of images and better average values of JSC (92.16%), DSC (94.05%), FPR (3.82%), FNR (2.73%), PRE (99.14%), F-M (99.50%), SEN (99.91%), SPE (97.88%), and ACC (98.04%) are obtained.

Table 7. Performance assesment using BraTS 2013 dataset.

Furthermore, the efficiency of the proposed tumor segmentation tool is validated against other brain segmentation procedures existing in the literature, such as Particle Swarm Optimization assisted Otsu and Markov Random Field (Otsu+MRF) segmentation (Palani et al., 2016), bat algorithm assisted Kapur and active contour (Kapur+AC) segmentation (Madhuvanthi et al., 2017), region growing technique (Węgliński and Fabijańska, 2011), and principal component analysis (Zhang and Wu, 2012). The performances of these methods are evaluated based on the computational cost (measured using Matlab's Tic-Toc function) and the segmented tumor similarity with respect to the ground truth image. For this investigation, two axial view slices of pseudo data name 0027 of BraTS 2013 dataset depicted in Table 8 is considered. The experimental result offers the average computation cost of 48.17sec (proposed),

53.74sec (Otsu+MRF), 84.19sec (Kapur+AC), 77.46sec (region growing), and 50.18sec (PCA). In which, the Kapur+AC and region growing approaches are semi-automated procedures, requires the operator's assistance for initiation. The computation time of the proposed approach is comparatively smaller than the alternatives, which ensures its throughput. The results available in Table 9, Figure 4 and 5 also confirm the advantage of Tsallis + MRF technique.

Table 8. Validation of the proposed procedure with other existing methods.

Table 9. Statistical measure values

Procedure	Image	SEN	SPE	ACC
Otsu+MRF	Slice_100	0.9825	0.7315	0.8478
	Slice_120	0.9975	0.6576	0.8099
Kapur+AC	Slice_100	0.9984	0.8328	0.9119
	Slice_120	0.9995	0.8762	0.9358
Region growing	Slice_100	0.9996	0.7961	0.8921
	Slice_120	0.9998	0.8915	0.9441
PCA	Slice_100	0.9987	0.8534	0.9232
	Slice_120	0.9987	0.8731	0.9338
Proposed Tsallis+MRF	Slice_100	0.9973	0.9580	0.9774
	Slice_120	0.9957	0.9759	0.9858

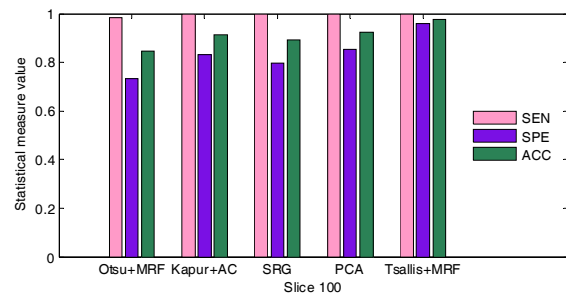Fig. 4 Performance evaluation for Slice_100
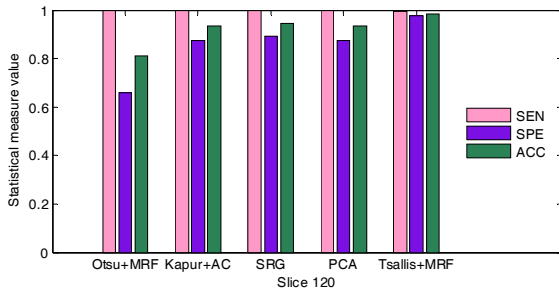
Fig. 5. Performance evaluation for Slice_120.

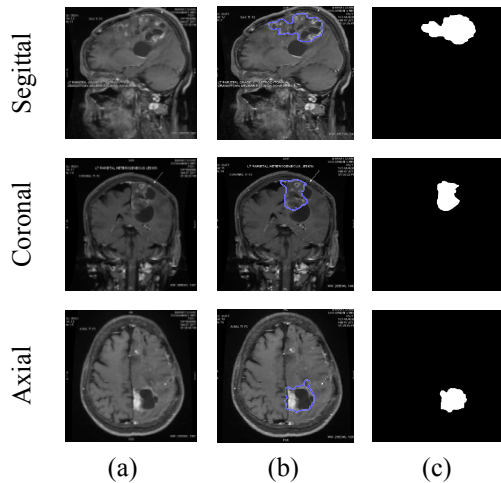(a)   (b)   (c)

Fig. 6. Clinical test data of BERF. (a) Test image, (b) Ground truth, (c) Extracted tumor.

In order to evaluate the clinical significance of Tsallis+MRF technique, real patient's database (512 x 512 size) collected from Bharat Education and Research Foundation (BERF) is considered. The three views of the sample test images are depicted in Fig 6 (a) along with its ground truth as in Fig 6(b). The suspicious region of the test images are extracted using the proposed approach as in Fig 6 (c). The experimental study confirms that, the proposed approach work well on the real time clinical data and also offers better values of image similarity measures, such as JSC (86.36%), DSC (91.34%), SEN (97.86%), SPE (92.82%), and ACC (96.83%). From this study, it can be observed that, the FA assisted Tsallis + MRF approach can be used to analyze the brain MR images regardless of its size, modality and orientation.

4. CONCLUSION

In this paper, Firefly Algorithm assisted segmentation and analysis of brain tumor is demonstrated by considering 2D gray scale brain MR images obtained from the benchmark and clinical dataset. It is an automated procedure and effectively extracts the tumor mass from the MRI dataset obtained using various modalities, such as T1, T2 and Flair. This technique is also tested on various views of the brain MRI. The proposed approach is grouped in to two sections, namely the pre-processing region and the post-processing region. The experimental result shows that, both the methods offer better result for the considered dataset. The competence of the proposed segmentation procedure is validated using the BraTS dataset. Results of this study exhibit that, the segmented tumor mass is approximately similar to the ground truth image and offers better result in normalized area, JSC, DSC, FPR and FNR for the T1, T2 and Flair MRI dataset. The advantage of the proposed approach is validated against existing approaches, such as Otsu + MRF, Kapur's + AC, seed based region growing, and principal component analysis. The computed accuracy measures confirms that, Tsallis+MRF approach offers better result compared with the alternatives considered in this paper. Finally, the clinical significance of the Tsallis+MRF approach is evaluated using the real patient's MR images collected from Bharat Education and Research Foundation.

REFERENCES

Abdel-Maksoud, E., Elmogy, M. and Al-Awadi, R. (2015). Brain tumor segmentation based on a hybrid clustering technique, *Egyptian Informatics Journal*, vol.16, pp. 71–81.

Agrawal, S., Panda, R., Bhuyan, S. and Panigrahi, B.K. (2013). Tsallis entropy based optimal multilevel thresholding using cuckoo search algorithm, *Swarm and Evolutionary Computation*, Vol. 11, pp. 16–30.

Akay, B. (2013). A study on particle swarm optimization and artificial bee colony algorithms for multilevel thresholding, *Applied Soft Computing*, Vol.13, pp.3066–3091.

Balafar, M.A., Ramli, A.R., Saripan, M.I. and Mashohor, S. (2010). Review of brain MRI image segmentation methods, *Artificial Intelligence Review*, Vol.33, pp. 261–274.

Bhandari, A.K., Kumar, A. and Singh, G.K. (2015). Modified artificial bee colony based computationally efficient multilevel thresholding for satellite image segmentation using Kapur's, Otsu and Tsallis functions, *Expert Systems with Applications*, Vol. 42, No. 3, pp. 1573–1601.

Chaddad, A. and Tanougast, C. (2016) Quantitative evaluation of robust skull stripping and tumor detection applied to axial MR images, *Brain Informatics,* Vol.3, No.1, pp.53-61.

Chaddad, A. (2015) Automated Feature Extraction in Brain Tumor by Magnetic Resonance Imaging Using Gaussian Mixture Models, *International Journal of Biomedical Imaging*, Vol. 2015, Article ID 868031, 11 pages.

Despotovic, I., Goossens, B. and Philips, W. (2015) MRI Segmentation of the Human Brain: Challenges, Methods, and Applications, *Computational and Mathematical Methods in Medicine*, Vol.2015, Article ID 450341, 23 pages.

Elazab, A., Wang, C., Jia, F., Wu, J., Li, G. and Hu, Q. (2015). Segmentation of Brain Tissues from Magnetic Resonance Images Using Adaptively Regularized Kernel-Based Fuzzy C -Means Clustering,

Computational and Mathematical Methods in Medicine, Vol. 2015, Article ID 485495, 12 pages.

Grgic, S., Grgic, M. and Mrak, M. (2004). Reliability of objective picture quality measures, *Journal of Electrical Engineering*, Vol. 55, No. 1-2, pp. 3–10.

Jianjun, Z., Jixiang, R. and Shi, Q. (2012). Unsupervised Brain MRI Segmentation Using Improved Expectation-Maximization Algorithm, Advances in Technology and Management, AISC 165, pp. 785–792.

Jobin Christ, M.C. and Parvathi, R.M.S. (2012). A Survey on MRI Brain Segmentation, *Advances in Computer Science, Eng. & Appl.*, AISC 166, pp.167–177.

Jung, H.Y. and Lee, K.M. (2015). Image Segmentation by Edge Partitioning over a Nonsubmodular Markov Random Field, *Mathematical Problems in Engineering*, vol. 2015, Article ID 683176, 9 pages.

Kai Chen, Yifan Zhou, Zhisheng Zhang, Min Dai, Yuan Chao. and Jinfei Shi. (2016) Multilevel Image Segmentation Based on an Improved Firefly Algorithm, *Mathematical Problems in Engineering*, Vol. 2016, Article ID 1578056, 12 pages.

Kamalanand, K. and Ramakrishnan, S. (2015). Effect of Gadolinium Concentration on Segmentation of Vasculature in Cardiopulmonary Magnetic Resonance Angiograms, *Journal of Medical Imaging and Health Informatics*, Vol. 5, pp.1–5.

Khandani, M.K., Bajcsy, R. and Fallah, Y.P. (2009). Automated Segmentation of Brain Tumors in MRI Using Force Data Clustering Algorithm, *Lecture Notes in Computer Science,* Vol. 5875, pp. 317–326.

Kistler, M., Bonaretti, S., Pfahrer, M., Niklaus, R. and Büchler, P. (2013). The Virtual Skeleton Database: An Open Access Repository for Biomedical Research and Collaboration, *Journal of Medical Internet Research*, Vol.15, No.11, e245.

Larobina, M., Murino, L., Cervo, A. and Alfano, B. (2015). Self-Trained Supervised Segmentation of Subcortical Brain Structures Using Multispectral Magnetic Resonance Images, *Bio Med Research International*, Vol. 2015, Article ID 764383, 9 pages.

Lu, H., Kot, A.C. and Shi, Y.Q. (2004). Distance-reciprocal distortion measure for binary document images, *IEEE Signal Processing Letters*, Vol. 11, No. 2, pp. 228-231.

Lu, Y., Wang, J., Kong, J., Zhang, B. and Zhang, J. (2006). An Integrated Algorithm for MRI Brain Images Segmentation, *Lecture Notes in Computer Scienc,* Vol. 4241, pp.132 – 142.

Madhuvanthi, S., Madhumathi, K., Deepa, P. and Sri Madhava Raja, N. (2017). A Soft-computing Assisted Tool to Detect and Analyse Brain Tumor, *International Journal of Engineering and Technology,* Vol.9, No.2, pp. 1341-1348.

Manickavasagam, K., Sutha, S. and Kamalanand, K. (2014). Development of Systems for Classification of Different Plasmodium Species in Thin Blood Smear Microscopic Images, *Journal of Advanced Microscopy Research*, Vol.9, No.2, pp. 86-92.

Menze et al., (2015). The Multimodal Brain Tumor Image Segmentation Benchmark (BRATS), *IEEE Transactions on Medical Imaging,* Vol. 34, No.10, pp.1993-2024.

Moghaddam, R.F. and Cheriet, M. (2010). A multi-scale framework for adaptive binarization of degraded document images, *Pattern Recognition*, vol.43, No.6, pp. 2186-2198.

Palani, T.K., Parvathavarthini, B. and Chitra, K, (2016). Segmentation of Brain Regions by Integrating Meta Heuristic Multilevel Threshold with Markov Random Field, *Current Medical Imaging Reviews*, Vol.12, No.1, pp. 4-12.

Raja, N.S.M., Arockia Sukanya, S. and Nikita, Y.(2015). Improved PSO Based Multi-level Thresholding for Cancer Infected Breast Thermal Images Using Otsu, *Procedia Computer Science*, Vol. 48, pp. 524-529.

Raja, N.S.M., Kavitha, G. and Ramakrishnan, S. (2012). Analysis of vasculature in human retinal images using particle swarmoptimizatio based tsallis multi-level thresholding and similarity measures, *Lecture Notes in Computer Science*, Vol. 7677, pp. 380–387.

Raja, N.S.M., Rajinikanth,V. and Latha, K. (2014). Otsu Based Optimal Multilevel Image Thresholding Using Firefly Algorithm, *Modelling and Simulation in Engineering*, Vol. 2014, Article ID 794574,17 pages.

Raja, N.S.M., Suresh Manic, K. and Rajinikanth, V. (2013). Firefly algorithm with various randomization parameters: an analysis, *Lecture Notes in Computer Science*, Vol. 8297, pp. 110–121.

Rajesh Sharma, R. and Marikkannu, P. (2015). Hybrid RGSA and Support Vector Machine Framework for Three-Dimensional Magnetic Resonance Brain Tumor Classification, *The Scientific World Journal*, Vol. 2015, Article ID 184350, 14 pages.

Rajinikanth, V. and Couceiro, M.S. (2015). RGB Histogram Based Color Image Segmentation Using Firefly Algorithm, *Procedia Computer Science*, Vol. 46, pp. 1449-1457.

Sathya, P.D. and Kayalvizhi, R.(2010). Optimum multilevel image thresholding based on Tsallis Entropy method with bacterial foraging algorithm, *International Journal of Computer Science Issues*, Vol. 7, No. 5, pp. 336–343.

Tsallis, C. (1988). Possible generalization of Boltzmann-Gibbs statistics, *Journal of Statistical Physics*, Vol. 52, pp.479–487.

Tuba, M. (2014). Multilevel image thresholding by nature-inspired algorithms: A short review, *Computer Science Journal of Moldova*, Vol.22, No.3, pp. 318-338.

Wang, Z., Bovik, A.C., Sheikh, H.R. and Simoncelli, E.P. (2004). Image Quality Assessment: From Error VisibilitytoStructural Similarity, *IEEE Transactions on Image Processing*, Vol. 13, No. 4, pp. 600 – 612.

Węgliński, T. and Fabijańska, A. (2011). Brain tumor segmentation from MRI data sets using region growing approach, in Proceedings of the 7th International Conference on Perspective Technologies and Methods in MEMS Design (MEMSTECH '11), pp. 185–188.

Yang, X.-S. (2009). Firefly algorithms formultimodal optimization, in Stochastic Algorithms: Foundations and Applications, *Lecture Notes in Computer Science*, Vol. 5792, pp. 169–178.

Yazdani, S., Yusof, R., Karimian, A., Riazi, A.H. and Bennamoun, M. (2015). A Unified Framework for Brain

Segmentation in MR Images, *Computational and Mathematical Methods in Medicine*, Vol. 2015, Article ID 829893, 17 pages.

Yushkevich, P.A., Piven, J., Hazlett, H.C., Smith, R.G., Ho, S., Gee, J.C. and Gerig, G. (2006). User-guided 3D active contour segmentation of anatomical structures: Significantly improved efficiency and reliability. *Neuroimage*, Vol.31, No.3, pp.1116-1128.

Zhang, Y., Brady, M. and Smith, S. (2001). Segmentation of brain MR images through a hidden Markov random field model and the expectation maximization algorithm, *IEEE Transactions on Medical Imaging*, Vol.20, No.1, pp. 45–57.

Zhang, Y. and Wu, L. (2012). An MR brain images classifier via principal component analysis and kernel support vector machine, Progress In Electromagnetics Research, Vol. 130, pp.369-388.

Brain Tumor Database (BRAINIX), http://www.osirix-viewer.com/datasets/

Brain Tumor Database (BraTS-MICCAI), http://hal.inria.fr/hal-00935640.

Software to read 3D brain images (http://www.itksnap.org/pmwiki/pmwiki.php)

BERF (http://www.bharatscans.com/)